Piezo-optic coefficients of MgO-doped $LiNbO_3$ crystals

Bogdan G. Mytsyk,[1] Anatoliy S. Andrushchak,[2] Nataliya M. Demyanyshyn,[1] Yaroslav P. Kost',[1] Andriy V. Kityk,[3,*] Pietro Mandracci,[4] and Wilfried Schranz[5]

[1]Karpenko Physico-Mechanical Institute, 5 Naukova Street, 79601 Lviv, Ukraine

[2]Lviv Polytechnic National University, 12 Stepana Bandera Strasse, 79013 Lviv, Ukraine

[3]Institute for Computer Science, Department of Electrical Engineering, Czestochowa University of Technology, Al. Armii Krajowej 17, PL-42200 Czestochowa, Poland

[4]Politecnico di Torino, Materials Science and Chemical Engineering Department, Materials and Microsystems Laboratory, corso Duca degli Abruzzi 24, 10129 Torino, Italy

[5]Faculty of Physics, University of Vienna, Boltzmanngasse 5, A-1090 Vienna, Austria

*Corresponding author: kityk@ap.univie.ac.at

Received 12 January 2009; revised 19 February 2009; accepted 21 February 2009; posted 24 February 2009 (Doc. ID 106255); published 25 March 2009

We describe an interferometric technique suitable for determination of piezo-optic coefficients (POCs) in crystals. The method considers real nonparallelism of measured samples, thereby improving the measuring precision of POCs significantly. Corresponding equations are derived for the interferometric half-wave stress method. Using this technique we have determined a complete set of POCs of pure and MgO-doped $LiNbO_3$ crystals. The reliability of the data has been confirmed by comparing the effective POCs expressed through the combinations of measured POCs and the effective POCs determined independently using highly precise optical birefringence measurements. Pure and MgO-doped $LiNbO_3$ crystals reveal nearly the same magnitudes of POCs. However, $LiNbO_3$:MgO exhibits about 4 times higher resistance with respect to powerful light radiation, making it more suitable for application in acousto-optic devices that deal with superpowerful laser radiation.

OCIS codes: 120.3180, 160.4670, 160.1050, 120.4530.

1. Introduction

Precise determination of piezo-optic coefficients (POCs) is important in many aspects of materials science and optical engineering, especially when one searches for new efficient acousto-optic materials. With a complete set of POCs and elastic compliances the photoelastic constants p_{ij} may be evaluated [1–3]. Thus the diffraction efficiency defined by the figure of merit $M_2 = n^6 p^2/(\rho V^3)$ [4–6] can be determined for each particular geometry of acousto-optic interaction. Here V is the sound velocity, n is the refractive index, p is the effective photoelastic constant represented as a combination of p_{ij} depending on sample geometry, and ρ is the crystal density. Optimized geometries of acousto-optic interaction, which provide the best diffraction efficiency of acousto-optic cells, can be found by analyzing the spatial anisotropy of $M_2(\boldsymbol{\theta}, \varphi)$. A detailed description of the optimization procedure is given in our previous works [7,8].

In this paper we describe an interferometric technique suitable for measurements of POCs in crystal materials. The proposed new method accounts for real nonparallelism of measured samples, which significantly improves the precision of the determined

0003-6935/09/101904-08$15.00/0

POCs. Using such a technique, complete sets of POCs of pure and MgO-doped (7% in melt composition) $LiNbO_3$ crystals have been obtained. The interferometric method was afterward verified by comparing the obtained POCs with the effective piezo-optic constants. The latter constants, which represent combinations of POCs, have been determined for several symmetry-equivalent geometries using independent high-precision optical birefringence measurements. Our interest in MgO-doped $LiNbO_3$ crystals (hereafter also referred to as $LiNbO_3$:MgO) is due to their high resistance with respect to power laser radiation; according to Ref. [9] their resistance is about 4 times higher compared to pure $LiNbO_3$ crystals, which appears to be very important for many applications.

2. Determination of POCs in Crystal Materials: Description of the Method and Basic Equations

Measurements of POCs in crystal materials are usually related to certain difficulties and/or uncertainties leading in many cases to incorrect values for the following reasons [10]: (i) absence of a complete set of equations suitable for the determination of POCs by an interferometric technique that would take into account the elastic crystal deformation; (ii) with lower crystal symmetry the number of independent nonzero POCs increases, which significantly complicates such equations especially when elastic crystal deformation is considered; (iii) improper use of the refractive index factor in the elastic contribution. In several works this factor was taken as n_i instead of $n_i - 1$, resulting in a fatal error in determination of POCs; (iv) a sign uncertainty of POCs due to a sequence of sign uncertainties regarding the chosen axes that form the right crystallographic coordinate system (see Ref. [11]). These shortcomings have been improved in several works. For a detailed discussion see the review article [10] and the references in it. This article also presents the set of equations that are suitable for the determination of POCs for crystals of any symmetry via the measurements of a mechanical-stress-induced optical path.

First we describe the interferometric technique that has been applied for the determination of POCs π_{im} in trigonal $LiNbO_3$ crystals. Then the results of these measurements are compared with the effective piezo-optic constants π^*_{km} (i.e., combinations of POCs π_{im}) measured by a highly accurate optical-polarization technique. Here the indices m, k, and i denote the directions of uniaxial mechanical compression, light propagation, and electric field vector oscillation, respectively. They are defined in the crystallophysical coordinate system with the axes X_1, X_2, and X_3 that coincide with the principal axes of the optical indicatrix. By defining these indices we specify the orientation of the sample subjected to piezoinduced interferometry and, as in Ref. [11], we refer to a chosen set of indices as a *sample geometry*. The experimental setup is based on a Mach–Zehnder interferometer, which is assumed to be rigid enough that changes of the interference pattern should be formed due to an induced change of optical path in a crystal sample only. Accordingly, the interferometer must be free from any mechanical deformation, which has been verified by means of a steel cube ($\sim$10 mm$\times$ 10 mm $\times$ 10 mm) with a hole ($\varnothing \sim 5$ mm). It was placed instead of the sample in such a way that one of the interference beams passed freely through the hole. Uniaxial mechanical stresses up to 2000 N/cm^2 applied to the cube did not lead to any shift of interference maxima as required. Small rotations of the sample in both the horizontal and the vertical planes have been verified through a visual inspection of the laser beam reflected from the sample surface and then consequently removed by adjusting the sample holder orientation. However, the most serious problem appeared due to a micrometric parallel shift of the sample perpendicular to the laser beam. In this case even small nonparallelity of real samples may produce a considerable error in the determination of POCs. Therefore, we consider below the way to eliminate such errors in the interferometric piezo-optic measurements.

An induced change of the optical path $\Delta_k = n_i d_k$ caused by the uniaxial stress σ_m applied to a rectangular sample is given by the well-known relation [11]

$$\delta\Delta_k = -\frac{1}{2}\pi_{im}\sigma_m n_i^3 d_k + S_{km}\sigma_m d_k(n_i - 1), \qquad (1)$$

where d_k is the sample thickness in the direction of light propagation and S_{km} are the elastic compliancy tensor constants. The first term of Eq. (1) describes "purely" piezo-optic changes of the optical path, whereas the second term is caused by the sample deformation in the direction of light propagation. Equation (1) is valid only for perfect parallel faced samples. Real samples usually exhibit small nonparallelism of opposite faces, which can be characterized by the angle $\alpha \approx \tan\alpha = a/l$ (see Fig. 1). Let us try to estimate the error due to nonparallelism of the sample. Assuming that a is typically in the range of 5–10 μm for the sample with $l = 8$ mm one obtains $\alpha = (3.6 - 7.2) \times 10^{-2}$ deg. By applying the force $F_m = 1000$ N to the sample we usually obtain a vertical sample shift δl of about of 5×10^{-2} mm, thus the

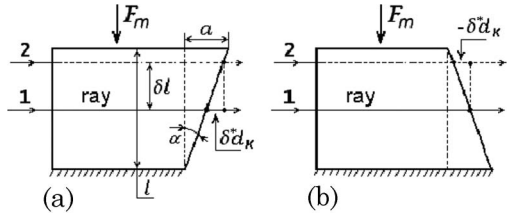

Fig. 1. Nonparallelism of the sample leads to an error $(\delta^* d_k)$ in the determination of the piezo-optic coefficients: 1 and 2 are the laser beam positions at $F_m = 0$ and $F_m \neq 0$, respectively. (a) Normal sample orientation and (b) inverted sample orientation (turned by 180° around the laser beam). By combining the normal and inverted sample orientations the error due to sample nonparallelism can be eliminated.

change of local sample thickness (i.e., along the line of the light beam propagation) $\delta^* d_k = a\delta l/l = 62.5\,\text{nm}$. For $LiNbO_3$:MgO crystals with $n_i = 2.28$ [9] this yields an absolute error in the determination of optical path changes of $\delta^*\Delta_k = n_i\delta^* d_k \approx 140\,\text{nm}$. For the light wavelength $\lambda = 632.8\,\text{nm}$ this is equivalent to a relative error of about 44%, assuming that the half-wave stress $\sigma_{\lambda/2} \approx F_m/S$, where S is the area of the sample faces to which the force F_m is applied. This error is proportionally larger for samples with higher magnitudes of the half-wave stress $\sigma_{\lambda/2}$.

For samples with perfectly parallel faces POCs π_{im} can be calculated using the equation

$$\pi_{im} = -\frac{\lambda}{\sigma_{im} n_i^3 d_k} + \frac{2S_{km}}{n_i^3}(n_i - 1), \tag{2}$$

where σ_{im} is the half-wave stress. This equation is directly obtained from Eq. (1) for $\delta\Delta_k = \lambda/2$ and $\sigma_m = \sigma_{im}$. To obtain a similar relation for the sample with nonparallel faces we must add the error correction $\delta^*\Delta_k$ to the right part of Eq. (1). Since the correction $\delta^*\Delta_k$ is unknown one must consider an alternative sample geometry [namely, a 180° turned sample as shown in Fig. 1(b)] to eliminate it. In this case the error correction $\delta^*\Delta_k$ must be subtracted from the right part of Eq. (1). For convenience, hereafter we will call the sample orientations shown in Figs. 1(a) and 1(b) *normal* and *inverted*, respectively. Combining both sample orientations, one obtains the equation [12]

$$\pi_{im} = -\frac{\lambda}{2n_i^3 d_k}\left(\frac{1}{\sigma_{im}} + \frac{1}{\sigma'_{im}}\right) + \frac{2S_{km}}{n_i^3}(n_i - 1), \tag{3}$$

where σ_{im} and σ'_{im} are the half-wave stresses measured for the normal [Fig. 1(a)] and inverted [Fig. 1(b)] sample orientations, respectively. It should be stressed that Eq. (3) is valid only for a set of principal POCs π_{im}, i.e., i, $m = 1, 2, 3$. The crystals $LiNbO_3$:MgO, like pure $LiNbO_3$, are characterized by the point group symmetry 3m. Thus their POC matrix contains additionally three nonprincipal POCs, π_{41}, π_{14}, and π_{44}. They can be determined by measuring the $X/45°$-cut sample (see Fig. 2). To determine π_{14} the sample geometry is defined as $i = 1$, $m = 4$, $k = \bar{4}$. For such a geometry the following relation is valid:

$$\pi_{14} + \pi_{12} + \pi_{13} = -\frac{\lambda}{n_1^3}\left(\frac{1}{d_{\bar{4}}\sigma_{14}} + \frac{1}{d_{\bar{4}}\sigma'_{14}}\right) + \frac{n_1 - 1}{n_1^3}(S_{11} + S_{33} - S_{44} + 2S_{13}), \tag{4}$$

where σ_{14} and σ'_{14} are the half-wave stresses measured for the normal and inverted sample orientations, respectively, and $d_{\bar{4}}$ is the sample thickness along the light beam propagation ($k = \bar{4}$). A similar

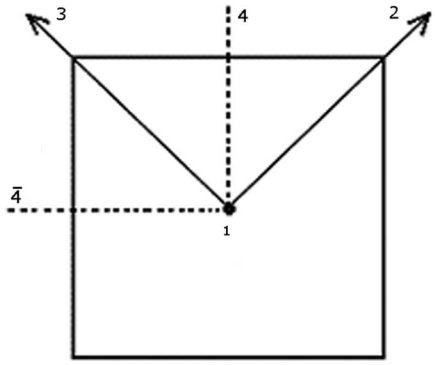

Fig. 2. Sample orientation required for the determination of POCs π_{14}, π_{41}, and π_{44}.

relation can also be written for the symmetrical experimental conditions ($i = 1$, $m = \bar{4}$, $k = 4$):

$$-\pi_{14} + \pi_{12} + \pi_{13} = -\frac{\lambda}{n_1^3}\left(\frac{1}{d_4\sigma_{1\bar{4}}} + \frac{1}{d_4\sigma'_{1\bar{4}}}\right) + \frac{n_1 - 1}{n_1^3}(S_{11} + S_{33} - S_{44} + 2S_{13}). \tag{5}$$

Determination of π_{14} by means of Eq. (4) or Eq. (5) is tainted by an extended set of errors, related in particular to the determination of half-wave stresses σ_{14} and σ'_{14} ($\sigma_{1\bar{4}}$ and $\sigma'_{1\bar{4}}$); elastic compliances S_{11}, S_{33}, S_{44}, and S_{13}; refractive indices n_i; π_{12} and π_{13}; and sample thickness d_4 ($d_{\bar{4}}$). Standing alone these equations are not very suitable for a precise determination of POC π_{14}. However, by mutual subtraction of Eq. (5) from Eq. (4) one obtains the relation

$$\pi_{14} = -\frac{\lambda}{2n_1^3}\left(\frac{1}{\sigma^0_{14}} + \frac{1}{\sigma'^0_{14}} - \frac{1}{\sigma^0_{1\bar{4}}} - \frac{1}{\sigma'^0_{1\bar{4}}}\right), \tag{6}$$

which considerably reduces the resulting error in determination of π_{14}. Here $\sigma^0_{im} = \sigma_{im} d_k (\sigma'^0_{im} = \sigma'_{im} d_k)$ is the so-called effective half-wave stress (i.e., the stress applied to a hypothetical cube sample with a volume of $1\,\text{cm}^3$ that induces retardation of $\lambda/2$).

In order to determine π_{41} one has to perform the measurements in direct ($i = 4$, $k = \bar{4}$, $m = 1$) and symmetrical ($i = \bar{4}$, $k = 4$, $m = 1$) conditions. The corresponding equation then takes the form

$$\pi_{41} = -\frac{\lambda}{4n_4^3}\left(\frac{1}{\sigma^0_{41}} + \frac{1}{\sigma'^0_{41}} - \frac{1}{\sigma^0_{\bar{4}1}} - \frac{1}{\sigma'^0_{\bar{4}1}}\right) - S_{14}\frac{n_4 - 1}{n_4^3}. \tag{7}$$

In this case the elastic contribution [second term of Eq. (7)] cannot be avoided, which increases the error in determination of π_{41}. POC π_{44} may also be obtained by performing the measurements in direct ($i = 4$, $k = \bar{4}$, $m = 4$) and symmetrical ($i = \bar{4}$, $k = 4$, $m = \bar{4}$) conditions:

$$\pi_{44}+\frac{1}{2}(\pi_{11}+\pi_{13}+\pi_{31}+\pi_{33})$$
$$=-\frac{\lambda}{2n_4^3}\cdot\left(\frac{1}{\sigma_{44}^0}+\frac{1}{\sigma_{44}'^0}+\frac{1}{\sigma_{\bar{4}4}^0}+\frac{1}{\sigma_{\bar{4}4}'^0}\right)$$
$$+(S_{11}+S_{33}-S_{44}+2S_{13})\cdot\frac{n_4-1}{n_4^3}. \quad (8)$$

However its determination is obviously characterized by a substantially larger error. More details regarding the errors in the interferometric piezo-optic measurements of $LiNbO_3$:MgO will be given in Section 4. Derivation of Eqs. (6)–(8) can be found in Ref. [12].

3. Reliability of POCs Determined by Interferometric Technique

The interferometric technique is known to be sophisticated, being critically sensitive to the quality of optical surfaces, residual strains in the sample, mechanical vibrations, random micrometric deformations, and/or shifts of interferometer components. These factors may have a considerable influence on the accuracy of interferometric measurements. Hence an independent verification of measured POCs is desirable whenever possible.

For example, π_{11} can be measured using several sample geometries. Considering the rectangular sample with the faces perpendicular to the principal crystallophysical axes X_1, X_2, and X_3, the sample geometry suitable for its determination can be assigned as $k=2$, $i=1$, and $m=1$. Hence Eq. (3) takes the form

$$\pi_{11}=-\frac{\lambda}{2n_1^3d_2}\left(\frac{1}{\sigma_{11}}+\frac{1}{\sigma_{11}'}\right)+2S_{21}\frac{(n_1-1)}{n_1^3}. \quad (9)$$

On the other hand, π_{11} can also be measured considering the sample geometry for which $k=3$, $i=1$, and $m=1$. In this case one obtains another relation quite similar to Eq. (9) in which d_2 and S_{21} are replaced by d_3 and S_{31}, respectively. π_{22}, which in the case of the symmetry group 3m is equal to π_{11}, can be determined using the two following sample geometries: $k=1$, $i=2$, $m=2$ or $k=3$, $i=2$, $m=2$. Accordingly, one obtains two additional relations suitable for the determination of π_{22}. The reliability of POCs determined by an interferometric technique can easily be verified by comparing the obtained magnitudes of π_{11} and π_{22}, which are expected to be equal to within experimental error.

Alternatively the magnitude of π_{11} can be obtained by measuring the piezoinduced optical path on the sample representing the $X/45°$ cut of $LiNbO_3$:MgO. The sample geometry must be chosen as $k=4$, $i=1, m=1$ (see Fig. 2), which leads to the expression

$$\pi_{11}=-\frac{\lambda}{2n_1^3d_4}\left(\frac{1}{\sigma_{11(k=4)}}+\frac{1}{\sigma_{11(k=4)}'}\right)$$
$$+\left(S_{12}+S_{13}+S_{14}\right)\frac{n_1-1}{n_1^3}. \quad (10)$$

Similarly, for symmetric conditions ($k=\bar{4}$, $i=1$, $m=1$) the following equation is valid:

$$\pi_{11}=-\frac{\lambda}{2n_1^3d_{\bar{4}}}\left(\frac{1}{\sigma_{11(k=\bar{4})}}+\frac{1}{\sigma_{11(k=\bar{4})}'}\right)$$
$$+(S_{12}+S_{13}-S_{14})\frac{n_1-1}{n_1^3}. \quad (11)$$

π_{11} can be determined by using Eqs. (10) and (11) or a superposition of these equations. In the last case the elastic compliancy S_{14} is eliminated, which improves the accuracy of the measurements a bit. Combining Eqs. (4) and (5), one obtains the expression for superposition of π_{12} and π_{13}:

$$\pi_{12}+\pi_{13}=-\frac{\lambda}{2n_1^3}\left(\frac{1}{d_{\bar{4}}\sigma_{14}}+\frac{1}{d_{\bar{4}}\sigma_{14}'}+\frac{1}{d_4\sigma_{1\bar{4}}}+\frac{1}{d_4\sigma_{1\bar{4}}'}\right)$$
$$+(S_{11}+S_{33}-S_{44}+2S_{13})\frac{n_1-1}{n_1^3}. \quad (12)$$

In a similar way one gets two other relations for superpositions of π_{12} and π_{31} or π_{41} and $\pi_{14}/2$:

$$\pi_{12}+\pi_{31}=-\frac{\lambda}{2n_4^3}\left(\frac{1}{d_{\bar{4}}\sigma_{41}}+\frac{1}{d_{\bar{4}}\sigma_{41}'}+\frac{1}{d_4\sigma_{\bar{4}1}}+\frac{1}{d_4\sigma_{\bar{4}1}'}\right)$$
$$+2(S_{12}+S_{13})\frac{n_4-1}{n_4^3}, \quad (13)$$

$$\pi_{41}+\frac{1}{2}\pi_{14}=\frac{\lambda}{2n_4^3}\left(\frac{1}{d_{\bar{4}}\sigma_{44}}+\frac{1}{d_{\bar{4}}\sigma_{44}'}-\frac{1}{d_4\sigma_{\bar{4}\bar{4}}}-\frac{1}{d_4\sigma_{\bar{4}\bar{4}}'}\right). \quad (14)$$

Table 1 lists the sample geometries used in the study of POCs of $LiNbO_3$:MgO crystals as well as the magnitudes of the effective half-wave stresses σ_{im}^0 and $\sigma_{im}'^0$ obtained by means of an interferometry technique.

4. POCs of MgO-Doped $LiNbO_3$ Crystals

MgO-doped (7 wt. %) $LiNbO_3$ crystals have been obtained by the Czochralski technique combined with a monodomainization procedure at $T_m=1200$ °C. Slow cooling from T_m down to room temperature has provided a significant reduction of intrinsic strains and hence high optical quality of the single crystals of nearly cylindrical shape ($Ø\sim 84$ mm, $L=60$ mm). Samples with typical dimensions of ~8 mm × 8 mm × 8 mm have been cut from the central part.

Table 1. Results of Piezo-Optic Measurements of $LiNbO_3$:MgO Crystals in Different Sample Geometries[a]

Sample Geometry	m		k	i	σ^0_{im} and σ'^0_{im}, kg/cm^2		π_{im}, Br	$\frac{\delta\Delta_k}{d_k\sigma_m}$, Br	$\frac{\delta\Delta_k(\pi_{im})}{\delta\Delta_k}$ (%)	$\frac{\delta\Delta_k(S_{km})}{\delta\Delta_k}$(%)
1	1	1′	2	1	$\sigma^0_{11} = -205$	$\sigma'^0_{11} = -225$	$\pi_{11} = -0.50 \pm 0.03$	+1.5	+200	−100
2	1	1′	2	3	$\sigma^0_{31} = +87$	$\sigma'^0_{31} = +76$	$\pi_{31} = +0.50 \pm 0.08$	−4.0	+66	+34
3	1	1′	3	1	$\sigma^0_{11} = -500$	$\sigma'^0_{11} = -500$	$\pi_{11} = -0.40 \pm 0.02$	+0.66	+360	−260
4	1	1′	3	2	$\sigma^0_{21} = +123$	$\sigma'^0_{21} = +110$	$\pi_{21} = +0.18 \pm 0.05$	−2.8	+38	+62
5	2	2′	1	2	$\sigma^0_{22} = -390$	$\sigma'^0_{22} = -325$	$\pi_{22} = -0.40 \pm 0.02$	+0.92	+260	−160
6	2	2′	1	3	$\sigma^0_{32} = +76$	$\sigma'^0_{32} = +90$	$\pi_{32} = +0.49 \pm 0.07$	−3.95	+65	+35
7	2	2′	3	1	$\sigma^0_{12} = +132$	$\sigma'^0_{12} = +129$	$\pi_{12} = +0.13 \pm 0.04$	−2.5	+31	+69
8	2	2′	3	2	$\sigma^0_{22} = -450$	$\sigma'^0_{22} = -470$	$\pi_{22} = -0.41 \pm 0.02$	+0.72	+340	−240
9	3	3′	1	2	$\sigma^0_{23} = +50$	$\sigma'^0_{23} = +54$	$\pi_{23} = +0.76 \pm 0.10$	−6.25	+72	+28
10	3	3′	1	3	$\sigma^0_{33} = +90$	$\sigma'^0_{33} = +101$	$\pi_{33} = +0.34 \pm 0.06$	−3.4	+53	+47
11	3	3′	2	1	$\sigma^0_{13} = +66$	$\sigma'^0_{13} = +41$	$\pi_{13} = +0.79 \pm 0.10$	−6.4	+73	+27
12	3	3′	2	3	$\sigma^0_{33} = +125$	$\sigma'^0_{33} = +85$	$\pi_{33} = +0.30 \pm 0.06$	−3.2	+50	+50
13	1	1′	4	1	$\sigma^0_{11} = -420$	$\sigma'^0_{11} = -650$	$\pi_{11} = -0.47 \pm 0.03$	+0.6	+470	−370
14	1	1′	4	$\bar{4}$	$\sigma^0_{41} = +41$	$\sigma'^0_{41} = +36$	$\pi_{41} = -0.95 \pm 0.09$	−9.7	+79	+21
15	1	1′	$\bar{4}$	1	$\sigma^0_{11} = -215$	$\sigma'^0_{11} = -235$	$\pi_{11} = -0.41 \pm 0.03$	+1.4	+174	−74
16	1	1′	$\bar{4}$	4	$\sigma^0_{41} = -96$	$\sigma'^0_{41} = -104$	$\pi_{41} = -0.85 \pm 0.18$	+1.45	+168	−68
17	4	4′	$\bar{4}$	1	$\sigma^0_{14} = +160$	$\sigma'^0_{14} = +125$	$\pi_{14} = -0.80 \pm 0.11$	−3.25	+12	+88
18	4	4′	$\bar{4}$	4	$\sigma^0_{44} = +27$	$\sigma'^0_{44} = +21$	$\pi_{44} = +2.0 \pm 0.5$	−13.7	+79	+21
19	$\bar{4}$	$\bar{4}$′	4	1	$\sigma^0_{1\bar{4}} = +48$	$\sigma'^0_{1\bar{4}} = +24$	$\pi_{14} = -0.80 \pm 0.11$	−8.0	+64	+36
20	$\bar{4}$	$\bar{4}$′	4	$\bar{4}$	$\sigma^0_{\bar{4}4} = +53$	$\sigma'^0_{\bar{4}4} = +48$	$\pi_{44} = +2.0 \pm 0.5$	−6.5	+56	+44

[a] + and − at σ^0_{im} and σ'^0_{im} indicate the sign of the optical path change under the stress σ_m applied to the sample (at calculations this sign is set before λ); sample compression is taken with −. For a synonymous choice of the directions $4\,i\,\bar{4}$ we use the criteria $\pi_{14} < 0$, then the signs of the crystallophysical axes are chosen according to IRE standards (see Ref. [11]).

The magnitudes of elastic compliances used in evaluations of POCs of $LiNbO_3$:MgO crystals have been taken from Ref. [13]: $S_{11} = 5.71$, $S_{12} = -1.13$, $S_{13} = -1.36$, $S_{33} = 4.82$, $S_{14} = -0.89$, $S_{44} = 16.65$ (given in $10^{-12}\,\mathrm{m}^2/\mathrm{N}$). The principal refractive indices ($\lambda = 633\,\mathrm{nm}$) $n_1 = n_2 = 2.282$, $n_3 = 2.192$ are taken from Ref. [9], whereas the magnitudes of the effective refractive index n_4 (or $n_{\bar{4}} = n_4$) required for the determination of π_{41} and π_{44} have been calculated using the known equation

$$n_4 = \sqrt{2} n_1 \cdot n_3 / \sqrt{n_1^2 + n_3^2} = 2.236.$$

Accordingly, for the sample geometries with $k = 1$ and $k = 4$ the birefringence values are $\Delta n_1 = n_2 - n_3 = 0.090$ and $\Delta n_4 = \Delta n_{\bar{4}} = n_1 - n_4 = 0.046$, respectively.

Table 1 summarizes the measured effective half-wave stresses depending on the sample geometry as well as the determined POCs of $LiNbO_3$:MgO crystals. We do not present here the analogous data for the pure $LiNbO_3$ crystals because they are very close to the ones obtained for $LiNbO_3$:MgO. The POCs averaged over the different sample geometries are given in Table 2 for both pure and MgO-doped crystals. For comparison, this table also contains the magnitudes of the POCs of pure $LiNbO_3$ published earlier in Ref. [14]. In the following we discuss the obtained results, including their reliability, error analysis, and practical aspects.

1. The reliability of the obtained data follows from the independent geometries used for the determination of the same POCs. For example, π_{11} (or $\pi_{22} = \pi_{11}$) has been calculated using Eq. (9), being the basic expression for the four independent sample geometries related to measurements of the rectangular sample with the faces perpendicular to the principal crystallophysical axes; see rows 1, 3, 5, and 8. Additionally, π_{11} has been obtained by measuring a rectangular sample of the $X/45°$ cut in two sample geometries (rows 13 and 15) and calculated by means of Eqs. (10) and (11), respectively. All other POCs of $LiNbO_3$:MgO have been determined at least from two independent measurements performed for different sample geometries: $\pi_{12} = \pi_{21}$ (rows 4 and 7), $\pi_{32} = \pi_{31}$ (rows 2 and 6), π_{14} (rows 17 and 19), etc. For the symmetry-equivalent sample geometries the corresponding POCs π_{im} exhibit very close magnitudes. Deviation from the mean value does not exceed 15%. Regarding POC measurements, such accuracy can be highly appreciated.

Table 2. POCs π_{im} of $LiNbO_3$:MgO and $LiNbO_3$ Crystals[a]

π_{im}, Br	π_{11}	π_{12}	π_{13}	π_{31}	π_{33}	π_{14}	π_{41}	π_{44}
$LiNbO_3$: MgO	−0.43	+0.15	+0.78	+0.50	+0.32	−0.80	−0.90	+2.0
$LiNbO_3$	−0.38	+0.09	+0.80	+0.50	+0.20	−0.81	−0.88	+2.25
$LiNbO_3$[b]	−0.47	+0.11	+2.0	+0.47	+1.6	+0.7	−1.9	+0.21

[a] The POC magnitudes are averaged over different symmetry-equivalent sample geometries.
[b] Ref. [14].

By means of Eqs. (12) and (13) one can calculate the superposition of the principal POCs $\pi_{12}+\pi_{13}$ and $\pi_{12}+\pi_{31}$ using the magnitudes of effective half-wave stresses σ^0_{14}, $\sigma^0_{1\bar{4}}$, and σ^0_{41}, $\sigma^0_{\bar{4}1}$, respectively, measured on the $X/45°$-cut sample. One obtains $\pi_{12}+\pi_{13}=0.61\pm0.15$ and $\pi_{12}+\pi_{31}=0.43\pm0.10$ (in Brewsters, $1\,\mathrm{Br}=10^{-12}\,\mathrm{m^2/N}$), which differ less than 20% from the corresponding magnitudes presented in Table 1. The superposition $\pi_{41}+\pi_{14}/2$ determined by means of Eq. (14) yields a value of $-1.25\pm0.12\,\mathrm{Br}$, which differs by only $\pm2\%$ from the one calculated using the values of Table 1.

2. The results of these comparisons confirm the reliability of the obtained results in $LiNbO_3$:MgO. The accuracy of POCs given in Table 1 ranges from 5% (as for π_{11}) up to 31% (as for π_{12}). These errors were calculated as the sum of mean-square deviations caused by the pure piezo-optic and elastic contributions according to Eq. (2). The relative error rises considerably if these contributions are comparable and have opposite signs.

3. From Table 1 it follows that piezo-optic $\delta\Delta_k(\pi_{im})$ and elastic $\delta\Delta_k(S_{km})$ contributions are comparable in most cases. Only the sample geometry used for the determination of π_{14} (see row 17 of Table 1) is characterized by an extremely small piezo-optic contribution ($\sim$12%) being comparable with the experimental error. Hence the optical path changes induced by the stress are dominated in this case by indirect elastic contribution. Amazingly in several cases both piezo-optic and elastic contributions exceed several times the resulting piezo-optic effect defined by their difference (see, e.g., row 8 or 13 of Table 1).

4. From a practical point of view, e.g., for photoelastic modulators [15–17], there is considerable interest in those sample geometries that are characterized by large piezo-induced changes of the optical path $\delta\Delta_k$. For pure and MgO-doped $LiNbO_3$ there are six sample geometries that are characterized by significant stress derivatives of optical path $\delta\Delta_k/(\sigma_m d_k)$ in the range from –6.25 up to –13.7 Br (see rows 9, 11, 14, and 18–20 of Table 1).

5. Table 2 compares the magnitudes of POCs π_{im} of pure and MgO-doped crystals. The difference between corresponding coefficients appears within the experimental error. This is also the case for π_{33}, for which such a difference is comparable with the magnitude of this coefficient.

On the other hand, the magnitudes of several POCs, e.g., π_{13}, π_{33}, π_{41}, or π_{44}, show discrepancies with the ones determined earlier (see Table 2). We attribute such discrepancies to several reasons:

i. Possible nonparallelism of samples has not been taken into account in Ref. [14], which may lead to large errors in the determination of POCs.

ii. In our studies we used the same samples for interferometric (POCs π_{im}) and elastic (compliances S_{km}) measurements, whereas the authors of Ref. [14] used literature data on S_{km} magnitudes.

iii. A proper choice of positive directions in the crystallophysical coordinate system is very important. In the present work we followed IRE standards [18] developed for the piezoelectric effect. Accordingly, the coefficients π_{14} and S_{14} get negative magnitudes in contrast to Ref. [14] where they are both positive. It must be stressed that the IRE standard is generally accepted by most authors and is frequently used for characterization of acousto-optic efficiency.

Another verification of the data obtained by interferometric piezo-optic measurements can be performed by their comparison with the effective POCs determined by high-precision optical birefringence measurements. The effective POCs π^*_{km} are defined by the equation [11]

$$\pi^*_{km}=-\frac{2\delta(\Delta n_k)}{\sigma_m}=-\frac{2}{\sigma_m}(\delta n_i-\delta n_j), \tag{15}$$

where $\delta(\Delta n_k)$ is the piezoinduced optical birefringence and δn_i and δn_j are the changes of refractive indices expressed through POCs π_{im} as

$$\delta n_i=-\frac{1}{2}\pi_{im}\sigma_m n_i^3. \tag{16}$$

Inserting Eq. (16) into Eq. (15) leads to the relation between π^*_{km} and π_{im}:

$$\pi^*_{km}=\pi_{im}n_i^3-\pi_{jm}n_j^3, \tag{17}$$

where the indices k,i,j are related by the rule of cyclic permutation $(1-2-3-1\ldots)$. Equation (17) has been obtained in [2] and is valid only for the principal POCs π_{im} and π^*_{km}, i.e., where the indices i, k, $m=1,2,3$. For indices i, k, $m\geq4\,(\bar{4})$ the relations for the corresponding effective POCs π^*_{km} become more complicated. For instance, if the direction of light propagation is set as $k=4$ and the two orthogonal polarizations are defined accordingly as $i=\bar{4}$ and $j=1$ then one deals with POC $\pi^*_{km}=\pi^*_{4\bar{4}}$ expressed as

$$\pi^*_{4\bar{4}}=-\frac{2}{\sigma_{\bar{4}}}(\delta n_{\bar{4}}-\delta n_1), \tag{18}$$

where the indices k,i,j are related by the rule of cyclic permutation $1-4-\bar{4}-1\ldots$ [12]. The stress-induced changes of the refractive indices $\delta n_{\bar{4}}$ and δn_1 ($k=4$ and $m=\bar{4}$) are given by Ref. [11]:

$$\delta n_{\bar{4}}=-\frac{1}{8}(\pi_{11}+\pi_{13}+\pi_{14}+\pi_{31}+\pi_{33}+2\pi_{41}+2\pi_{44})\sigma_{\bar{4}}n_4^3, \tag{19}$$

$$\delta n_1=-\frac{1}{4}(\pi_{11}+\pi_{13}+\pi_{14})\sigma_{\bar{4}}n_1^3. \tag{20}$$

Table 3. Effective POCs π^*_{km} of $LiNbO_3$:MgO and $LiNbO_3$ Crystals[a]

	π^*_{km}, Br	π^*_{12}	π^*_{13}	π^*_{31}	π^*_{41}	$\pi^*_{\bar{4}1}$	$\pi^*_{4\bar{4}}$	$\pi^*_{\bar{4}4}$
$LiNbO_3$: MgO	Calculated from π_{im}	10.0 ± 0.9	5.9 ± 1.3	6.7 ± 0.6	18.8 ± 1.2	1.3 ± 1.2	3.1 ± 3.2	20.9 ± 3.2
	Determined from $\delta(\Delta n_k)/\delta\sigma_m$ [b]	10.2	6.1	6.7	19.5	2.1	2.2	22.5
$LiNbO_3$	Calculated from π_{im}	9.9 ± 0.9	7.4 ± 1.4	5.6 ± 0.5	17.8 ± 1.1	2.0 ± 1.1	1.6 ± 2.1	22.6 ± 2.1
	Determined from $\delta(\Delta n_k)/\delta\sigma_m$ [b]	9.6	7.6	5.6	16.6	1.85	2.3	19.8

[a] The π^*_{km} magnitudes are obtained by averaging over different symmetry-equivalent sample geometries.
[b] Ref. [19].

Hence by inserting Eqs. (19) and (20) into Eq. (18) one obtains the following equation for the effective POCs $\pi^*_{4\bar{4}}$:

$$\pi^*_{4\bar{4}} = \frac{1}{4}\left(\pi_{11} + \pi_{13} + \pi_{14} + \pi_{31} + \pi_{33} + 2\pi_{41} + 2\pi_{44}\right) \times n_4^3 - \frac{1}{2}\left(\pi_{12} + \pi_{13} + \pi_{14}\right)n_1^3. \quad (21)$$

In a similar way one can derive the relations for the remaining effective POCs $\pi^*_{\bar{4}4}$, π^*_{41}, and $\pi^*_{\bar{4}1}$. The calculated magnitudes π^*_{km} for pure and MgO-doped $LiNbO_3$ crystals are given in Table 3 and compared with corresponding magnitudes determined independently by the high-precision optical polarization method through measuring the piezoinduced birefringence $\delta(\Delta n_k)$ [19] [see Eq. (15)]. The errors are given only for the effective POCs π^*_{km}, being calculated from POCs π_{im}. They increase substantially for nonprincipal effective POCs π^*_{km} because these tensor components are expressed through a large number of measured POCs π_{im}; see, e.g., Eq. (21). In several cases the absolute error is comparable or even exceeds (e.g., for $\pi^*_{4\bar{4}}$) the magnitudes of obtained effective POCs. On the other hand, for π^*_{km} measured by the optical polarization technique the errors are much smaller, i.e., less than 5–7%. Moreover the magnitudes of the principal effective POCs measured by different techniques coincide within the experimental error, which can be considered as another confirmation for the reliability of the POCs π_{im} obtained by the interference technique.

Doping of $LiNbO_3$ crystals by MgO does not lead to a considerable modification of their piezo-optic properties. From Table 3 it follows that the magnitudes of corresponding effective POCs π^*_{km} of pure and MgO-doped $LiNbO_3$ crystals are close to each other, and their deviations from the mean values appear within the experimental error. Also the sums of all the effective POCs in $LiNbO_3$ and $LiNbO_3$:MgO exhibit similar magnitudes, 67.0 and 66.7 Br, respectively. However, $LiNbO_3$:MgO is characterized by about 4 times higher resistance with respect to powerful light radiation, making it promising for future application in acousto-optic devices such as modulators and deflectors that deal with superpowerful laser radiation.

5. Conclusions

In conclusion we have presented an interferometric technique suitable for the determination of POCs in crystals. The method considers real nonparallelism of measured samples, which improves the measuring precision of POCs significantly. It has been applied to pure and MgO-doped $LiNbO_3$ crystals to study their piezo-optic properties. Corresponding equations are derived for a complete set of POCs being measured by the interferometric half-wave stress method. Using such a technique we have determined a complete set of POCs of $LiNbO_3$ and $LiNbO_3$:MgO (7% in melt composition) crystals. The method has been verified by comparing the effective POCs expressed through the combinations of measured POCs and the effective POCs determined independently using high-precision optical birefringence measurements. The reliability of the data obtained by interferometric technique has been confirmed. Doping of $LiNbO_3$ crystals by MgO does not lead to a considerable modification of their piezo-optic properties, however $LiNbO_3$:MgO is known to exhibit considerably higher resistance against powerful light emission, which indeed defines a perspective for its application in acousto-optic devices that deal with superpowerful laser radiation.

This work has been supported by Science and Technology Center in Ukraine (STCU) project No. 4584.

References

1. J. F. Nye, *Physical Properties of Crystals* (Clarendon, 1985), p. 329.
2. A. S. Sonin and A. S. Vasilevskaya, *Electro-Optic Crystals* (Atomizdat, 1971), p. 327 [in Russian].
3. G. Kloos, "On photoelastic and quadratic electrostrictive effect," J. Phys. D **30**, 1536–1539 (1997).
4. N. Uchida and N. Niizeki, "Acousto-optic deflection materials and techniques," Proc. IEEE **61**, 1073–1094 (1973).
5. I. M. Silvestrova, A. V. Vinogradov, A. V. Shygorin, T. N. Turskaya, G. S. Belikova, and Ya. V. Pisarevskiy, "Elastic, piezoelectric, acousto-optic and non-linear optical properties of caesium ortosulphobenzoat crystals," Kristallografiya **35**, 906–911 (1990) [in Russian].
6. D. F. Nelson, *Electric, Optic and Acoustic Interactions in Dielectrics* (Wiley-Interscience, 1979), p. 539.
7. A. S. Andrushchak, Ya. V. Bobitski, M. V. Kaidan, B. V. Tybinka, A. V. Kityk, and W. Schranz, "Spatial anisotropy of photoelastic and acousto-optic properties in $\beta - BaB_2O_4$ crystals," Opt. Mater. **27**, 619–624 (2004).
8. A. S. Andrushchak, Ya. V. Bobitski, M. V. Kaidan, and B. V. Tybinka, "Spatial analysis of isotropic and anisotropic diffraction of light by transverse acoustic waves in barium betaborate crystals," Ukr. J. Phys. **50**, 26–33 (2005).
9. D. Yu. Sugak, A. O. Matkovskii, I. M. Solskii, B. M. Kopko, V. Ya. Oliinyk, I. V. Stefanskii, V. M. Gaba, V. V. Grabowskii, I. M.

Zaritskii, and L. G. Rakitina, "Growth and optical properties of $LiNbO_3$: MgO single crystals," Cryst. Res.Technol. **32**, 805–811 (1997).
10. B. Mytsyk, "Methods for the studies of the piezo-optic effect in crystals and the analysis of experimental data. II. Analysis of the experimental data," Ukr. J. Phys. Opt. **4**, 105–118 (2003).
11. B. Mytsyk, "Methods for the studies of the piezo-optic effect in crystals and the analysis of experimental data. I. Methodology for the studies of piezo-optic effect," Ukr. J. Phys. Opt. **4**, 1–26 (2003).
12. B. H. Mytsyk, A. S. Andrushchak, and G. I. Gaskevich, "Comprehensive studies of piezo-optic effect in langasite crystals," Ukr. J. Phys. Opt. **52**, 800–809 (2007).
13. H. P. Laba, O. V. Yurkevych, I. D. Karbovnyk, M. V. Kaidan, S. S. Dumych, I. M. Solskii, and A. S. Andrushchak, "Spatial anisotropy of electro-, piezo- and acousto-optic effects in crystalline materials of solid electronics. Approbation on example of $LiNbO_3$ and $LiNbO_3$:MgO part II. Completing of elastic and piezoelectric coefficients matrix for $LiNbO_3$ and $LiNbO_3$: MgO crystals," Herald Lviv Polytechnic National Univ. (Electronics) **619**, 172–180 (2008).
14. B. H. Mytsyk, Ya. V. Pryriz, and A. S. Andrushchak, "The lithium niobate piezo-optic features," Cryst. Res. Technol. **26**, 931–940 (1991).
15. M. N. Trainer, "Photoelastic measuring transducer and accelerometer based thereon," U.S. patent 4,648,274 (3 October 1997).
16. F. Brandi, E. Polacco, and G. Ruoso, "Stress-optic modulator," Meas. Sci. Technol. **12**, 1503–1508 (2001).
17. A. S. Andrushchak, B. H. Mytsyk, and B. V. Osyka, "Photoelastic stress transduser," USSR patent 1,796,936, published in Bulletin No. 7 (1993).
18. Yu. I. Syrotin and M. P. Shaskolskaya, *Fundamentals of Crystal Physics* (Nauka, 1979).
19. B. H. Mytsyk, A. S. Andrushchak, Ya. P. Kost', and I. M. Solskii, "Piezooptic effect in $LiNbO_3$:MgO crystals," J. Phys. Stud. **12**, 3702/1–3702/5 (2008).